Proceedings of the Eleventh Asian Congress of Fluid Mechanics
22-25 May 2006, Kuala Lumpur, Malaysia

PREDICTING THE FLOW STRESSES IN A SIMPLIFIED BIOREACTOR

B.T. Tan [Tan.Boon.Thong@eng.monash.edu.my] and Keith Liow
School of Engineering
Monash University Malaysia, 46150 Petaling Jaya, Malaysia

K. Hourigan, J. Sheridan and M.C. Thompson
Department of Mechanical Engineering
Monash University, 3800 Clayton, Australia.

ABSTRACT: The axisymmetric flow in a simplified bioreactor is simulated in this study. Next we analyse the stresses experienced by the fluid as a result of the mechanical agitation of the bioreactor. Statistical measurements are made with the aim of predicting the stress histories of cells cultured in bioreactors.

1. INTRODUCTION

Numerous studies have shown the importance of hydrodynamic forces when culturing biological cells in *in vitro* condition. The level of fluid shear stress levels have been found to affect the shape, orientation, proliferation rates or the production of certain chemicals. This has been observed in various mammalian cells such as endothelial cells (Davies, 1995), osteoblas cells (McDonald *et al.*, 1996) and chondrocytes cells (Guilak *et al.*, 2002).

Although there are numerous ways to mechanically stimulate cells *in vitro*, fluid shear systems have received considerable attention because they can more closely represent the *in vivo* environment. Bioreactors are the most common system used for this purpose. These are essentially mixing vessels which is agitated either by a mixing impeller or a magnetic stir-bar. It is well known that these rigs can produce complex flow fields in either the laminar or turbulent flow regime.

The flow field and the resultant mechanical stress levels experienced by cell cultures in a basic bioreactor is the focus of this study. The simplified design with a rotating bottom surface is used in this study. This reduces the system to one geometric parameter (i.e. the aspect ratio, h/r). The fluid is assumed to be homogeneous and Newtonian. The range of Reynolds numbers in this study are all within the laminar and steady flow regime.

Passive tracer particles are placed within the flow to simulate the convection of individual cells. This assumes that the cells do not affect the flow and is valid when the mass fractions of cells are low. The stress history of these particles are then recorded and the statistical quantities calculated. The data is used to gauge the mechanical stimulation experienced by the cells.

Figure 1(a) shows the schematic of the bioreactor with all the relevant dimensions. This system comprises of a circular flask or radius r. It is filled with fluid up to a height h and has a free surface on the top boundary. Two aspect ratios are considered in this study, namely $h/r = 1.5$ and 2.0. The rotational speed of the base is ω. The Reynolds number in this study is defined as,

$$Re = \frac{\rho \omega r^2}{\mu}, \tag{1}$$

where μ is the dynamic viscosity and ρ is the fluid density. The Reynolds number is varied between $500 \leq Re \leq 2400$ in this study.

2. NUMERICAL METHODS

This section is divided into three parts. Firstly the method used to quantify the forces experienced by a cell suspended in the fluid is presented. This is followed by a description of the numerical technique used to simulate the flow. Finally, the details involved in generating the statistics is discussed.

2.1 THE HYDRODYNAMIC FORCES

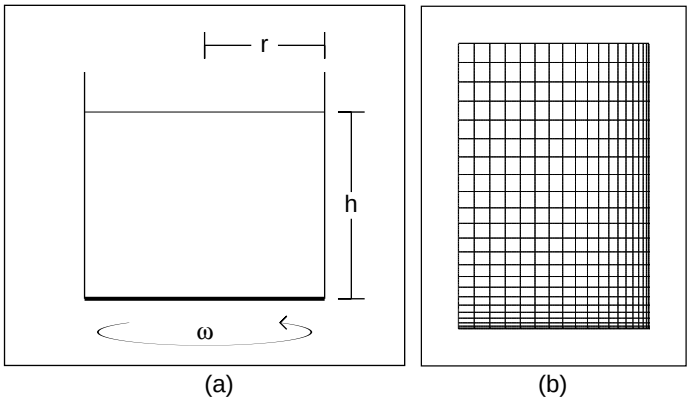

Figure 1: (a) A schematic of the simplified bioreactor and (b)a plot of the computational mesh showing the macro elements for $h/r = 1.5$.

Previous studies have quantitatively measured the shear stress applied to the cell growth medium and observed the associated cell culture (Dewey *et al.*, 1981 and Smith *et al.*. 1995). Special devices such cone-plate apparatus or viscometers are generally used for this purpose. These devices are designed to ensure that the entire sample experiences a constant and uniform amount of shearing in one direction. This is essentially achieved by shearing a thin film of fluid between two solid surfaces.

This method of quantifying does not easily extend to cells in a three-dimensional growth medium. The forces on the surface of a cell can be described by the viscous stress tensor when we neglect the effects of pressure. In three-dimensional space, this results in a stress tensor with 9 components which reduce to a symmetric tensor with 6 independent components for a Newtonian fluid. Croughan *et al.* (1987) only measured the shear component on two dimensional slices and therefore only captured one component of the stress tensor. Chalmers (2000) propoesed considering the entire stress tensor. Begley and Kleis (2000) vectorially summed the three non-diagonal elements and used this as their metric. This method is dependent on the selection of co-ordinate axis.

In this study, the principle stresses are used to measure the stresses experienced by the cells. They are independent of the coordinate axes, and are representative of the anisotropic component of the forces experienced by the cell walls at that particular location. The magnitude and direction of the principle stresses are found by calculating the eigenvalue and the eigenvector of the viscous stress tensor respectively. They are grouped into te most positive ($\sigma_(+ ve)$) which relates to tension, intermediate ($\sigma_(0)$) and most negative (($\sigma_(- ve)$).

2.2 FLOW SIMULATION

The flow is assumed to be axi-symmetric at the low Reynolds numbers considered in this study. This has been supported by experimental observations (Dusting *et al.*,2005). This reduces the problem to two spatial dimensions because there is no variations in the azimuthal direction. The free-surface on the top boundary is assumed to remain flat and free of deformation. This is valid for low Froude numbers. Experiments using water in a flask with $r = 32.5mm$ which is representative of a laboratory size bioreactor and within the Reynolds number range examined here also showed no surface deformation (Dusting *et al.*, 2005).

The flow field is modeled by solving the incompressible time-dependent Navier-Stokes equation in cylindrical polar coordinates. A spectral-element method is used for the axi-symmetric geometry and the solution is advanced in time using a time splitting technique that is second order accurate. This technique has been validated and is extensively used for various problems in both Cartesian and cylindrical polar space (Thompson, Lewek & Provansal, 2001 and Sheard, Thompson & Hourigan 2003).

A plot of the computational mesh used in this study is shown in Figure 1(b). The centreline in this plot and all preceding plots are on the left boundary. The mesh is stretched using the half Chebyshev (cosine) function toward the bottom and side walls where the gradients are largest. The grid used for $h/r = 2.0$ has several more elements in the vertical direction so that the size of the first cell from the bottom is approximately the same as when $h/r = 1.5$. Each macro element in this plot contain a further 10×10 computational nodes. A velocity profile is imposed on bottom boundary to represent a constant rotational rate of ω. A no slip boundary condition is imposed on the right boundary. At the free surface and centreline boundary, the velocity component normal to the boundary is set to zero and the normal

gradients of pressure and the velocity component tangential to the boundary is also set to zero.

Simulations are generally started with the solution from a lower Reynolds number case when one is available. The simulations are then integrated forward in time using a time step of $\omega\Delta t = 0.01$ for $Re \leq 1400$, and $\omega\Delta t = 0.005$ for cases with higher Reynolds number. All cases considered in this study asymptotes to steady state. Simulations starting with a solution from a lower Reynolds number typically require a few hundred time units to reach a steady asymptotic state. The flow is considered to be steady when the largest variation in any component of velocity at any node is less than $\frac{\Delta u}{\Delta t \omega^2 r} < 1e^{-6}$. Simulations were performed at higher spatial resolutions and using smaller time steps to verify the accuracy of the data.

2.3 TRACKING PARTICLES

Passive tracer particles are tracked and their stress histories were recorded for statistical analysis. This simulates the convection of biological cells in the reactor and the mechanical stimulation that it experiences. Firstly, the methods used to simulate the particle movement is discussed. The next part of this section explains the method used to generate the statistical data from a large number of particles.

The movement of the particle were simulated using two different methods. The first and simpler way is to assume that the particle "follows" the flow. The position of the particle, $\mathbf{x}_p$, at any time in the future can be calculated by integrating the following equation.

$$\mathbf{x}_p = \int \mathbf{u} dt. \tag{2}$$

$\mathbf{u}$ is the velocity vector of the flow field at the current particle position.

The other technique solves for the changes in momentum of the particle. The drag, pressure, added mass and boyancy forces are considered. The chosen parameters reflects the typical experimetal setting. The diameter of the particles and the bioreactor are $8\mu m$ and $65mm$ respectively. The fluid medium has the properties of water and the specific gravity of the particles we varied between 0.95 and 1.05.

The fourth order Runge-Kutta method is used to integrate the equations governing the particles movement. The flow field in its asymptotic state is used as the medium convecting the particles. The flow velocities and pressure gradients are interpolated using the same spectral expansions as the flow solver. The time step used to advance the particle that "follow" the flow is $\omega\Delta t = 0.005$. The particles governed by forces used a much smaller time step of between $\omega\Delta t = 1.0 \times 10^{-6}$ and $\omega\Delta t = 5.0 \times 10^{e-7}$ for stability. In both cases, the accuracy in simulating the particles is better than the flow solver because a higher order scheme is used with a smaller time step.

Test showed that even after several thousand time units, the difference in particle paths were the same order as the numerical errors. Therefore the "follows" the flow method was used for this study. This method is computationally cheaper and allowed larger time steps to be taken.

A large number of particles were simulated over an extended period of time to get a statistically accurate result. The particles were initially equally distributed (by volume) across an axi-symmetric plane. Simulations were performed with 9,600 (i.e 80x120) and 12,800 (i.e. 80x160) particles for $h/r = 1.5$ and 2.0 respectively. The particles were simulated for $\omega t = 1,000$ and data was sampled every $\omega\Delta t = 0.125$. A simulation with more particles simulated over a longer period and sampled more frequently was performed to verify that these samples were statistically accurate. Simulations with more particles, using a higher sampling frequnecy and with longer time histories were performed to validate the statistics.

3. RESULTS AND DISCUSSION

Results from the flow field simulations are presented first. This is followed by some statistical description such as mean and standard deviation of the *principle* stresses experienced by the cells. The probability density function for a selection of cases is also presented to show the stress distribution and their link to regions in the flow.

3.1 FLOW FIELD

The primary flow in the azimuthal direction is dominated by the rotating bottom lid and the diffusion of momentum away from the bottom lid. The secondary flow also transports momentum away from the rotating lid. The secondary flow in the radial and axial direction is illustrated by contours of streamfunction on the plane normal to the azimuthal direction. Figure 2 shows these contours for flows at $Re = 500$, $1,000$ and $1,500$ at aspect ratio of $h/r = 1.5$. The predominant recirculation region which is flowing in the clockwise direction is represented by the lighter shades of gray with contouring levels at an interval of $\Delta\frac{\phi}{\omega} = 0.001$. The flow recirculating in the anti-clockwise direction is represented by the

darker shades. A finer contouring level of $\Delta\frac{\phi}{\omega} = 0.0001$ is used to highlight the weaker recirculation. In both cases, the darker shades represent an increase in magnitude for the streamfunction.

These plots show that a single recirculating region dominates the secondary flow. The average velocity component normal to the radial and axial plane is approximately 50 times less than maximum velocity at the driving lid. The close spacing between levels show that the recirculating flow speeds up close to the outer rotating boundary (i.e. bottom right of the plots). A region recirculating weakly in the opposite direction forms near the centreline as the Reynolds number is increased. This forms at $Re \approx 700$ and $Re \approx 1,000$ for $h/r = 1.5$ and $h/r = 2.0$ respectively. This feature can be seen in Figure 2 when the flow is at $Re = 1,000$. As the Reynolds number continues to increase, this region distorts and separates from the centreline as seen at $Re = 2,000$. This flow feature has been previously studied and classied as a type of vortex breakdown. (Dusting *et al.*, 2005, Brøns *et al.*, 2001).

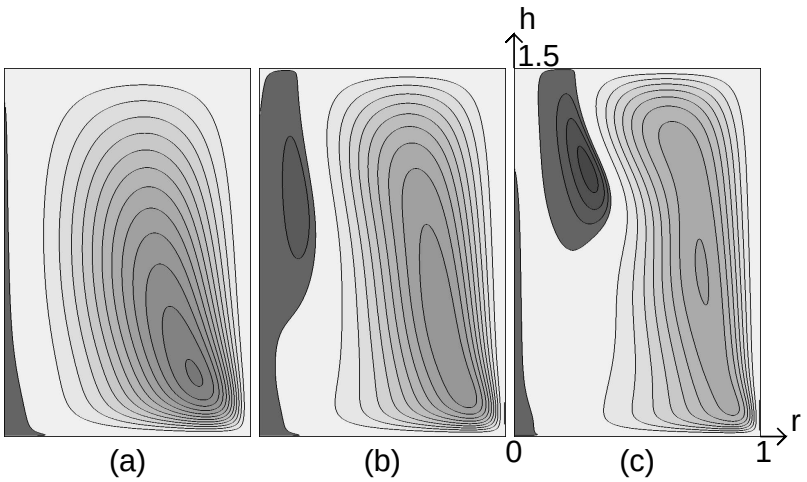

Figure 2: Contours of stream-function for (a) $Re = 500$, (b)$Re = 1000$ and (c)$Re = 2000$ in the $h/r = 1.5$ geometry.

3.2 PARTICLE TRACKING

A large number of particles are simulated to "follow" the flow over a long period of time. The *principle* stresses acting on each particle is recorded at constant time intervals. The most negative, intermediate and most positive *principle* stresses are grouped and analysed separately. The data is then used to generate statistics and probability distribution functions.

Overall Statistics

Flows with Reynolds number ranging between $500 \leq Re \leq 2400$ in both $h/r = 1.5$ and 2.0 geometries are analysed. Figure 3 shows the mean, median and standard deviation respectively for the most positive *principle* stresses as a function of flow Reynolds number. The statistics for the intermediate *principle* stresses are close to zero in this range of Reynolds numbers. The most negative *principle* stresses mirror that of the most positive *principle* stresses.

The same mechanism driving a larger volume of fluid results in the statistical measurements of stress levels being generally lower for the larger aspect ratio case. There is a small discontinuous increase in the overall trend around $Re = 700$ for $h/r = 1.5$ and $Re = 1,000$ for $h/r = 2.0$ in all three statistical quantities. This correspond to the onset of the recirculating region near the centreline as discussed earlier.

The large difference between the mean and median and the large values of standard deviations all imply that the probability distribution is highly skewed. The mean stress levels are relatively less sensitive to the flow Reynolds number. An increase in Reynolds number by a factor of approximately 5 changes the mean by approximately 25%. The median and standard deviation shows a larger variation (approximately 45%). This shows that the spread in *principle* stress levels increases with Reynolds number.

Probability Density Function

Figure 4 shows the probability distribution of the most positive principle stresses for the flows at $Re = 2000$ with aspect ratio, $h/r = 1.5$. The stress levels are distinguished by different shades of gray. Accompanying each of the graph is a contour plot where the stress levels can be matched to regions of the flow by the shades of gray. The principle stresses shows a highly skewed distribution which decays at

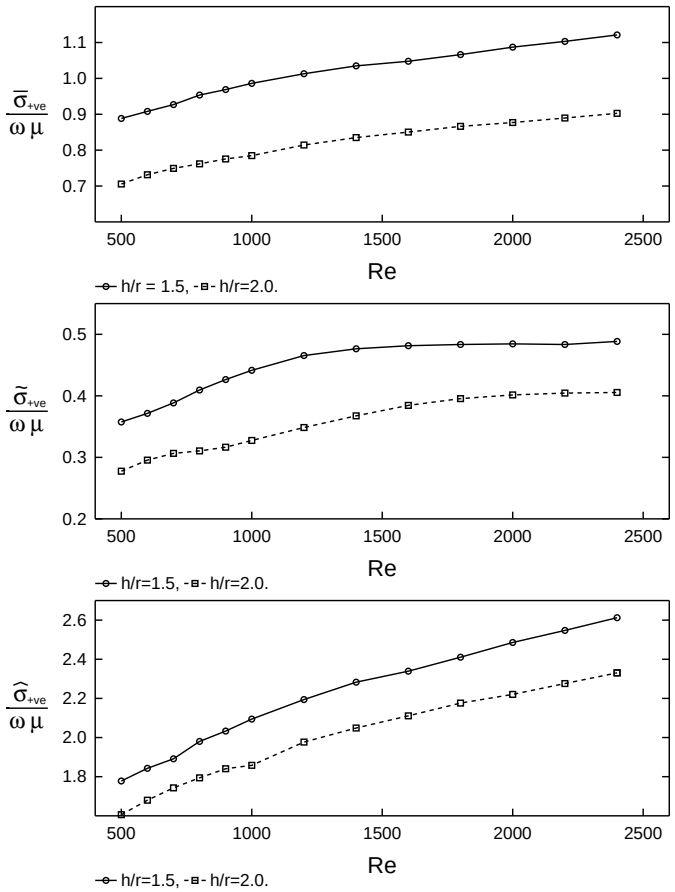

Figure 3: The mean and standard deviation of the maximum principle stresses experienced by particles in the flow.

larger magnitudes. The distribution shows a high concentration at the lower stress levels. The skewness is greater at lower Reynolds numbers. Exponential decay in the probability density function is observed when $\frac{\sigma_(-ve)}{\omega\mu} \lesssim -5.0$ and $\frac{\sigma_(+ve)}{\omega\mu} \gtrsim 5.0$

The *principle* stress distribution can be related to the features in the flow. The regions of high stresses are those close to the rotating boundary at the bottom and the outer wall boundary. This is associated with surfaces where momentum enters and leaves the system. The stress is also higher in the region close to the centreline and free surface. This region boarders the two recirculating regions of the secondary flow and is also the boundary of the vortex breakdown bubble. The stresses are relatively lower in the remainder of the system.

The probability density functions show several sharp peaks for all three principle stresses in every case. These peaks occur at relatively lower stress magnitudes for the most positive and negative principle stresses. These peaks are not due to an insufficiently large sample. Varying the sample size by changing the number of particles, sampling interval or total sampling time still produces identical peaks in the probability density function. These peaks corresponds to either region where the stress is relatively uniform (i.e. saddle or inflection points/regions) or regions where the particles move relatively slow. The location of these peaks are related to small features in the flow and therefore are sensitive to changes in the Reynolds number.

4. CONCLUSION

The flow in a simplified bioreactor is numerically simulated for a range of Reynolds number in the laminar flow regime. The *principle* stresses are used as a measure of the mechanical stimulus experienced by a cell. A large number of passive particles are simulated to "follow" the flow, and their stress histories are recorded. These are then used to obtain statistical description of the stresses experienced by a cell. The intermediate stress, σ_o, is negligible. The most negative (σ_{-ve}) and most (σ_{+ve}) positive stresses therefore mirror each other. The distribution is highly skewed. As the Reynolds number is increased,

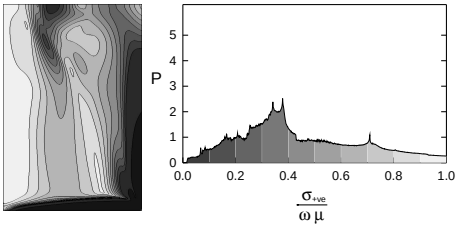

Figure 4: The probability distribution of most positive principle stress when $Re = 2,000$ for $h/r = 1.5$.

the mean stress level increases less relative to the standard deviation and median. The probability distribution plots show that the stress levels are concentrated to lower levels at low Reynolds numbers and the distributed to higher levels as the Reynolds number is increased. The distribution initially decays more rapidly and past $\frac{\sigma_(-ve)}{\omega\mu} \gtrsim -5.0$ or $\frac{\sigma_(+ve)}{\omega\mu} \lesssim 5.0$, the decay is exponential. The region of high stress include those near the rotating boundary, wall boundary and the region between the two recirculating region in the secondary flow representing the boundary of the vortex breakdown bubble.

5. ACKNOLEDGEMENTS

The first author would like to thank the Victorian Partnership for Advanced Computing (VPAC) Expertise Grant for their financial support.

References

[1] Aris, R., 1962. Vectors, tensors and basic equations of fluid mechanics, Prentice-Hall, Englewood Cliffs, N.J.

[2] Begley CM and Kleis SJ: The fluid dynamics and shear environment in the NASA/JSC rotating-wall perfused-vessel bioreactor. *Biotech. and Bioeng.* 2000,**70**(1), pp. 32-40.

[3] Brøns M, Voigt LK and Sørensen JN: Topology of vortex breakdown bubbles in a cylinder with a rotating bottom and a free surface. 2001,*J Fluid Mech.* **423**, pp. 133-148.

[4] Chalmers J: Animal cell culture, effects of agitation and aeration on cell adaptation in Encyclopedia of Cell Technology, R.E. Spier, Editor. John Wiley & Sons, New York. pp. 41-51, 2000.

[5] Croughan MS, Hamel J-F and Wang DIC: Hydrodynamic effects on animal cells grown in microcarrier cultures. *Biotech. and Bioeng.* 1987,**24**, pp. 130-141.

[6] Davies PF, Mundel T and Barbee KA: A mechanism for heterogeneous endothelial responses to flow *in vivo* and *in vitro*. *J of Biomech.* 1995, **28**(12), pp. 1553-1560.

[7] Dusting JC, Sheridan J, Hourigan K and Tan BT: Stresses in the Vortex Breakdown Region in Free Surface Lid-Driven Cylinder Flows. Submitted to *Phys. of Fluids (Letters)* 2005.

[8] Guilak F, Erickson GR and Ting-Beall HP: The effects of osmotic stress on the viscoelastic and physical properties of articular chondrocytes. *Biophys. J* 2002, **82**, pp. 720-727.

[9] McDonald F, Somasundaram B, McCann TJ, Mason WT and Meikle MC: Calcium waves in fluid flow stimulated osteoblasts are G protein mediated. *A of Biochem. and Biophys.* 1996, **326**(1), pp. 31-38.

[10] Sheard GS, Thompson MC and Hourigan K: From spheres to circular cylinders: classification of bluff ring transitions and structure of bluff ring wakes. *J Fluid Mech.*, 2003, **492**, pp. 147-180.

[11] Smith RL, Donlon BS, Gupta MK, Mohtai M, Das P, Carter DR, Cooke J, Gibbons G, Hutchinson N and Schurman DJ: Effects of fluid-induced shear on articular chondrocyte morphology and metabolism *in vitro*. *J Orthopaedic Res.* 1995, **13**(6), pp. 824-831.

[12] Thompson MC, Lewek Th and Provansal M: Kinematics and dynamics of sphere wake transition. 2001, *J Fluids and Struct.*, **15**, pp. 575-586.